# MedChemComm

Accepted Manuscript






ROYAL SOCIETY OF CHEMISTRY

www.rsc.org/medchemcomm

# A STEP FORWARD IN THE SIGMA ENIGMA: A ROLE FOR CHIRALITY IN THE SIGMA1 RECEPTOR-LIGAND INTERACTION? †

DANIELA ROSSI,[1#] ANNAMARIA MARRA,[1#] MARTA RUI,[1] ERIK LAURINI,[2] MAURIZIO FERMEGLIA,[2] SABRINA PRICL,[2,3] DIRK SCHEPMANN,[4] BERNHARD WUENSCH,[4] MARCO PEVIANI,[5] DANIELA CURTI,[5] SIMONA COLLINA[1*]

[1]*Department of Drug Sciences, Medicinal Chemistry and Pharmaceutical Technology section, University of Pavia, Viale Taramelli 12, 27100 Pavia (Italy)*

[2] *MOSE – DEA- University of Trieste Via Valerio 10, 34127 Trieste (Italy)*

[3] *National Interuniversity Consortium for Material Science and Technology (INSTM), Research Unit MOSE-DEA University of Trieste, Trieste, Italy*

[4]*Institute of Pharmaceutical and Medicinal Chemistry, University of Muenster, Correnstrasse 48, 48149 Muenster (Germany)*

[5]*Department of Biology and Biotechnology "L. Spallanzani", Laboratory of Cellular and Molecular Neuropharmacology, University of Pavia, Via Ferrata 9, 27100 Pavia (Italy)*

[#]These Authors contributed equally to this work.

[*]Correspondence to: Simona Collina, Department of Drug Sciences, Medicinal Chemistry and Pharmaceutical Technology section, University of Pavia, Viale Taramelli 12, 27100 Pavia (Italy). Phone: (+39)0382-987379, Fax: (+39)0382-422975. E-mail: simona.collina@unipv.it

†Electronic supplementary information (ESI) available: details of chemical synthesis, chiral resolution and absolute configuration assignment of compound **1**, and all details of molecular modeling study and biological investigation.

# A STEP FORWARD IN THE SIGMA ENIGMA: A ROLE FOR CHIRALITY IN THE SIGMA1 RECEPTOR-LIGAND INTERACTION?†

DANIELA ROSSI,[1#] ANNAMARIA MARRA,[1#] MARTA RUI,[1] ERIK LAURINI,[2] MAURIZIO FERMEGLIA,[2] SABRINA PRICL,[2,3] DIRK SCHEPMANN,[4] BERNHARD WUENSCH,[4] MARCO PEVIANI,[5] DANIELA CURTI,[5] SIMONA COLLINA[1*]

[1]*Department of Drug Sciences, Medicinal Chemistry and Pharmaceutical Technology section, University of Pavia, Viale Taramelli 12, 27100 Pavia (Italy)*

[2] *MOSE – DEA- University of Trieste Via Valerio 10, 34127 Trieste (Italy)*

[3] *National Interuniversity Consortium for Material Science and Technology (INSTM), Research Unit MOSE-DEA University of Trieste, Trieste, Italy*

[4]*Institute of Pharmaceutical and Medicinal Chemistry, University of Muenster, Correnstrasse 48, 48149 Muenster (Germany)*

[5]*Department of Biology and Biotechnology "L. Spallanzani", Laboratory of Cellular and Molecular Neuropharmacology, University of Pavia, Via Ferrata 9, 27100 Pavia (Italy)*

[#]These Authors contributed equally to this work.

[*]Correspondence to: Simona Collina, Department of Drug Sciences, Medicinal Chemistry and Pharmaceutical Technology section, University of Pavia, Viale Taramelli 12, 27100 Pavia (Italy). Phone: (+39)0382-987379, Fax: (+39)0382-422975. E-mail: simona.collina@unipv.it

**Abstract**

In our recent researches racemic **RC-33** was identified as a potent and highly promising $\sigma_1$ receptor agonist, showing excellent $\sigma_1$ receptor affinity and promoting NGF-induced neurite outgrowth in PC12 cell at very low concentrations. Surprisingly, both its interaction with the biological target and its effect on neurite sprouting proved to be non-stereoselective. Starting from the observation that an hydrogen bond center in the scaffold of a $\sigma_1$ ligand is an important pharmacophoric element for receptor/ligand interaction, we hypothesized that the absence of such pharmacophoric feature in the structure of **RC-33** could be also responsible for the lack of enantioselectivity in its interaction with the target receptor. To verify our hypothesis, in this paper we evaluated - both *in silico* and *in vitro* - the ability of a series of enantiomeric arylalkylaminoalcohols and arylpyrrolidinols **1-5** to interact with the receptor. All these compounds are structurally related to **RC-33** and characterized by the presence of an –OH group as the additional pharmacophore feature. Interestingly, the results of our study shows that the $\sigma_1$ receptor exhibits enantiopreference toward compounds characterized by (*S*)-configuration at the stereogenic center bearing the aromatic moiety only when the alcoholic group is also present at that chiral center, thus supporting our original hypothesis.

## Introduction

The sigma (σ) binding sites were originally defined and classified as opioid receptor subtypes.[1] Later investigations demonstrated that σ receptors were distinct from opioid and phencyclidine analogues, and since then at least two distinct σ receptor subtypes, designated $\sigma_1$ and $\sigma_2$,[2] have been pharmacologically characterized.[3-5] In particular, the $\sigma_1$ receptor subtype has been purified and cloned from several animal species and man.[6,7] $\sigma_1$ receptors are ubiquitously expressed in mammalian tissues and highly distributed in the central nervous system (CNS),[8-10] with the highest density found in the spinal cord, cerebellum, hippocampus, hypothalamus, midbrain, cerebral cortex, and pineal gland. Strong pharmacological evidences indicate that $\sigma_1$ receptors are involved in the pathophysiology of all major CNS disorders,[11] including mood disorders (anxiety[12] and depression[13]), psychosis and schizophrenia,[14] as well as drug addiction, pain,[15] and neurodegenerative diseases such as Parkinson's, Alzheimer's, and amyotrophic lateral sclerosis.[16] Moreover, from a biological perspective, the $\sigma_1$ receptors reside in the endoplasmic reticulum (ER) at the ER–mitochondria interface,[17] and they are unique ligand-regulated molecular chaperones[18–20] that can translocate to the plasma membrane or to other subcellular compartments under stressful conditions and/or pharmacological manipulation.

Ligands displaying preferential affinity for the $\sigma_1$ receptor subtype are (+)-benzomorphans such as (+)-pentazocine and (+)-N-allylnormetazocine (NANM, SKF-10,047), whereas haloperidol and 1,3-di-(2-tolyl)guanidine (DTG) exhibit high affinity for both receptor subtypes[21]. Since (+)-pentazocine shows a very low affinity for the $\sigma_2$ receptors, it represents the prototypical selective agonist used in its tritiated form to label $\sigma_1$ receptors. Several compounds endowed with $\sigma_1$ affinity and selectivity, characterized by different scaffolds, have been identified, e.g., arylalkylamine,[22a–f] benzooxazolones,[23] and spirocyclic pyranopyrazoles,[24] and different pharmacophore models for $\sigma_1$ receptor ligands have been published. All these models share the common features of a basic amino group and at least two hydrophobic substituents at the basic nitrogen atom.[25a-f] However, the last-generation, three-dimensional (3D) pharmacophore models[25c-f] are characterized by an additional pharmacophore requirement: an heterogroup the scaffold of the molecule able to perform an hydrogen bond interaction with the receptor counterpart. Actually, heteroatoms such as O or S are frequently present in very potent $\sigma_1$ ligands, bridging the aromatic component and the classic alkyl or cycloalkyl intermediate spacer linked to the basic nitrogen atom.[26,27]

In this scenario, our group designed and synthesized a large number of very interesting $\sigma_1$ receptor ligands.[22a-c] Among these, the most promising molecule is 1-[3-(1,1'-biphen)-4-yl]butylpiperidine (**RC-33**, Fig. 1), showing excellent $\sigma_1$ receptor affinity and agonistic profile in its racemic form, as

testified by its $K_i$ $\sigma_1$ value of 0.70±0.3 nM and by the potentiation of the NGF-induced neurite outgrowth in PC12 cell at very low concentrations.[22c-d]

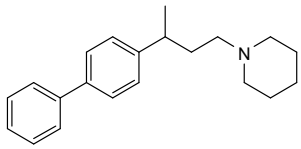

**Fig. 1.** (*R,S*)-**RC-33**

Racemic resolution of **RC-33** and isolation of the enantiomers revealed that i) the interaction with the biological target is non-stereoselective ($K_i\sigma_1^{(S)\text{- RC-33}}$ =1.9±0.2 nM, $K_i\sigma_1^{(R)\text{- RC-33}}$ =1.8±0.1 nM) and ii) the pharmacological activity is not dependent on the absolute configuration.[22e-f] The behavior of **RC-33** is particularly surprising, since the enantioselectivity of the $\sigma_1$ receptor is well documented.[20] Starting from the observation that an important pharmacophoric element is missing in the **RC-33** structure (i.e., an hydrogen bond donor or acceptor)[25c-e], we first hypothesized that the absence of such pharmacophoric feature could be responsible for the lack of enantioselectivity in the interaction with the biological target. Then, we verified our hypothesis by evaluating the ability of a series of enantiomeric arylalkylaminoalcohols and arylpyrrolidinols, structurally related to **RC-33**, to interact with $\sigma_1$ receptors. Specifically, here we report and discuss in detail the results of the *in silico* study, synthesis, chiral resolution and biological evaluation of the arylalkylaminoalcohol **1** (Table 1), analogue of **RC-33,** complemented by the *in silico* and *in vitro* study of other enantiomeric arylalkylaminoalcohol and arylpyrrolidinol derivatives (Table 1). These molecules were selected from a compound cohort previously prepared and characterized by us as analgesic agents with effects similar or higher than morphine but never evaluated as $\sigma_1$ receptor ligands.[28a-d]

The final aim of our work is to understand how chirality may affect the $\sigma_1$ receptor – ligand interaction and activity, thus contributing a step forward in unveiling the sigma-enigma. Indeed, even admittedly our knowledge of the sigma receptors has evolved over the past 20 years, several aspects in the sigma field still remain rather obscure.

## Results and Discussion

### Compound selection

With the aim of evaluating the role of a hydrogen bond center as an additional pharmacophore element in the stereoselective interaction with the $\sigma_1$ receptor we designed compound **1**, featuring an alcoholic function on the alkyl spacer bridging the aromatic ring to the basic nitrogen atom, as an analogue of the arylalkylamino derivative **RC-33** (Table 1).

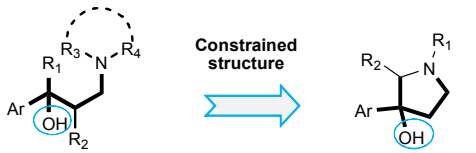


template **I** template **II**

| Compound | Template | Ar | $R_1$ | $R_2$ | $NR_3R_4$ |
|---|---|---|---|---|---|
| (*R,S*)-**1**<br>(*R*)-**1**<br>(*S*)-**1** | **I** | biphenyl-4yl | $CH_3$ | H | $N(CH_2)_5$ |
| (*R,S*)-**2**<br>(*R*)-**2**<br>(*S*)-**2** | **I** | naphth-2-yl | $CH_3$ | H | $N(CH_3)_2$ |
| (*R,S*)-**3**<br>(*R*)-**3**<br>(*S*)-**3** | **I** | 6-methoxy-naphth-2yl | $CH_3$ | H | $N(CH_3)_2$ |
| (*2R/S,3S/R*)-**4**<br>(*2R,3S*)-**4**<br>(*2S,3R*)-**4** | **II** | naphth-2yl | $CH_3$ | $CH_3$ | |
| (*2R/S,3S/R*)-**5**<br>(*2R,3S*)-**5**<br>(*2S,3R*)-**5** | **II** | 6-methoxy-naphth-2yl | $CH_3$ | $CH_3$ | |

**Table 1.** Alcoholic compounds structurally related to **RC-33**.

For the purpose of comparison and discussion, we selected other structurally related alcoholic compounds from our library of chiral molecules synthesized over the years. Among these, we chose molecules **2** and **3** (template **I,** Table 1) as structurally related to **1**, and the constrained arylpyrrolidinols **4** and **5** (template II, Table 1), being characterized by less conformational freedom.[28a,c,d]

**Synthesis, chiral resolution and configurational assignment**

For the synthesis of (*R,S*)-**1** we planned to follow the methodology described in our previous work, with suitable modifications (Scheme 1).[28a] We started our synthetic approach with the synthesis of 4-piperidinyl butan-2-one (**6**), obtained via Michael addiction from a solution of piperidine and but-3-en-2-one in PEG 400 in good yield (62%). Concerning the synthesis of (*R,S*)-**1**, β-aminoketone **6** was added to the biphenyl anion, obtained by halogen-metal exchange between aromatic substrate and *tert*-butyllitium (*tert*-BuLi) in anhydrous ethyl ether ($Et_2O$) at -40°C. After an acid-base work-up and purification by crystallization from methanol/water, (*R,S*)-**1** was obtained as white solid in good yield (68%). Final compound was characterized by $^1$H-NMR.

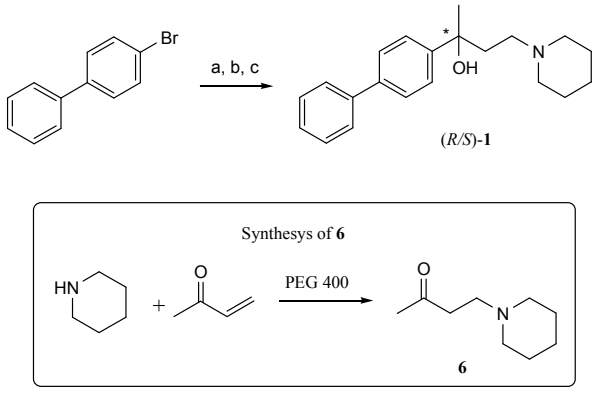


**Scheme 1.** Synthesis of (*R,S*)-**1**. Reagents and conditions: a) *t*-BuLi, anhydrous $Et_2O$, -40°C to rt; b) 4-piperidinyl butan-2-one (**6**), -78°C to 0°C; c) $H_2O$ rt.

In order to make (*R,S*)-**1** suitable for biological assays, a small amount of this compound was obtained in its salt form as (*R,S*)-**1**·**DL-tartrate**.

Chiral resolution of (*R,S*)-**1** was performed using chiral high performance liquid chromatography (HPLC). To identify the best experimental condition for the subsequent scaling-up, a standard screening protocol for cellulose and amylose derived chiral stationary phases (CSPs) was applied to the Chiralcel OJ-H (4.6 mm diameter x 150 mm length, 5µm), Chiralpak AS-H (4.6 mm diameter x 250 mm length, 5µm) and Chiralpak IC (4.6 mm diameter x 250 mm length, 5µm) columns, whose chiral selectors are cellulose *tris*-(4-methylbenzoate) (Chiralcel OJ-H) and amylose tris [(*S*)-α-methylbenzylcarbamate] (Chiralpak AS-H) coated on a silica gel substrate and cellulose tris (3,5-dichlorophenylcarbamate) immobilized on silica gel (Chiralpak IC). Elution conditions adopted included mixtures of *n*-heptane and polar modifiers (EtOH or 2-propanol), alcohols (MeOH, EtOH, and 2-propanol), and acetonitrile; in all cases 0.1% of diethylamine was added to the mobile phase; in the analysis with Chiralpak IC 0.3% of trifluoroacetic acid was also added. The best result, in terms of enantioselectivity (α) and resolution factor ($R_S$), was obtained with Chiralcel OJ-H, eluting with MeOH/diethylamine (100/0.1, v/v), as clearly illustrated in Fig. 2 ($t_{r1}$ = 6.99 min; $t_{r2}$ = 9.59 min; α = **1.98**; $R_S$ = **6.93**).

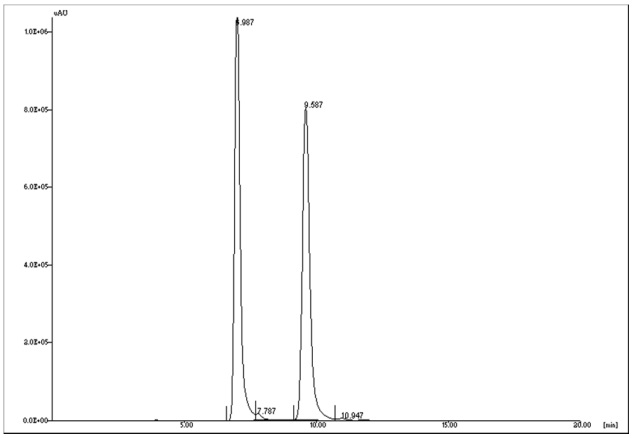


**Fig. 2.** Analytical separation of (*R,S*)-**1**. Chromatographic conditions: Chiralcel OJ-H (4.6 mm x 150 mm, 5µm ), MeOH/diethylamine 100/0.1 (v/v), flow rate: 0.5 mL/min, UV detector at 254 nm.

These experimental conditions are characterized by the most important prerequisites for an economic and productive enantiomeric separation on a semi-preparative scale, such as high solubility of racemate and enantiomers in the eluent solvent, shortest retention times, and the use of a mobile phase consisting of a pure low-cost solvent, which ultimately facilitates workup and re-use of the mobile phase. Therefore, the analytical method was suitably transferred to the semi-preparative scale employing Chiralpak OJ-H column (10 mm x 250 mm, 5 µm). In 17 cycles, 51 mg of (*R,S*)-**1** were processed, yielding 22.1 mg of the first eluted enantiomer and 23.2 mg of the second eluted one, characterized by $[\alpha]_D^{20}$ values of +24.1 and -24.2, respectively (c: 0.5 in MeOH), along with 5.7 mg of an intermediate fraction as a mixture of the two enantiomers. Both enantiomers of **1** were obtained with a yield of about 87 % and *ee* ≥ 99.9%, as evidenced by analytical control of the collected fractions.

The configuration assignment study of the resolved enantiomers of compound **1** was then performed comparing the electronic circular dichroism (ECD) curves of (+)-**1** with that of (*S*)-(-)-**2**, whose absolute configuration was already assigned.[28a] The ECD spectra (reported in the Supporting Information) of both (+)-**1** and (*S*)-(-)-**2** evidenced a similar profile in the range of wavelength between 200 and 300 nm. In detail, both compounds show a negative Cotton Effect (CE) at about 210 nm [(+)-**1**: $\lambda_{max}$ 206.5 nm, Mol.CD -6.61; (*S*)-(-)-**2**: $\lambda_{max}$ 209.0 nm, Mol.CD -6.21] and a positive CE in the range 220-260nm [(+)-**1**: $\lambda_{max}$ 253.5 nm, Mol.CD +2.60; (*S*)-(-)-**2**: $\lambda_{max}$ 224.0 nm, Mol.CD +16.80]. Based on these considerations, the absolute configuration (*S*) was assigned to (+)-**1.** Both enantiomers of **1** were finally converted into the corresponding tartrates [(*R*)-**1·L-tartrate** and (*S*)-**1·D-tartrate**, respectively], suitable for biological investigations.

**Molecular modeling studies**

Molecular Dynamics (MD) simulations were carried out to predict binding mode, affinity, and eventual stereoselective binding features of the selected compounds towards the $\sigma_1$ receptors. To the purpose, both (*R*) and (*S*) enantiomers of compounds **1-5** were modeled and the relevant free energy of binding ($\Delta G_{bind}$) with the protein was estimated via MM/PBSA calculations[29a,b] using the optimized structure of the compounds in complex with our validated homology model of the $\sigma_1$ receptor.[30a,b]

Taking compounds (*R*)-**1** and (*S*)-**1** as proof-of-concept, the analysis of the corresponding MD trajectories revealed that four major types of interactions are involved in the binding mode of both (*R*)-**1** and (*S*)-**1** to the $\sigma_1$ receptor, as showed in Fig. 3A and 3B: i) a permanent salt bridge is detected between the $-NH^+$ moiety of the ligand piperidine ring and the $COO^-$ group of Asp126; ii) the side chains of Arg119 and Trp121 are engaged in stabilizing $\pi$ interactions with the biphenyl group of the ligands; iii) several further hydrophobic interactions concur to stabilize compound/receptor binding, mainly via the side chains of the $\sigma_1$ residues belonging to the hydrophobic pocket Ile128, Phe133, and Tyr173; and iv) an hydrogen bond (HB) between the hydroxyl group of the compounds and the carboxylic chain of Glu172 conclusively anchors the ligand to the protein binding cavity.

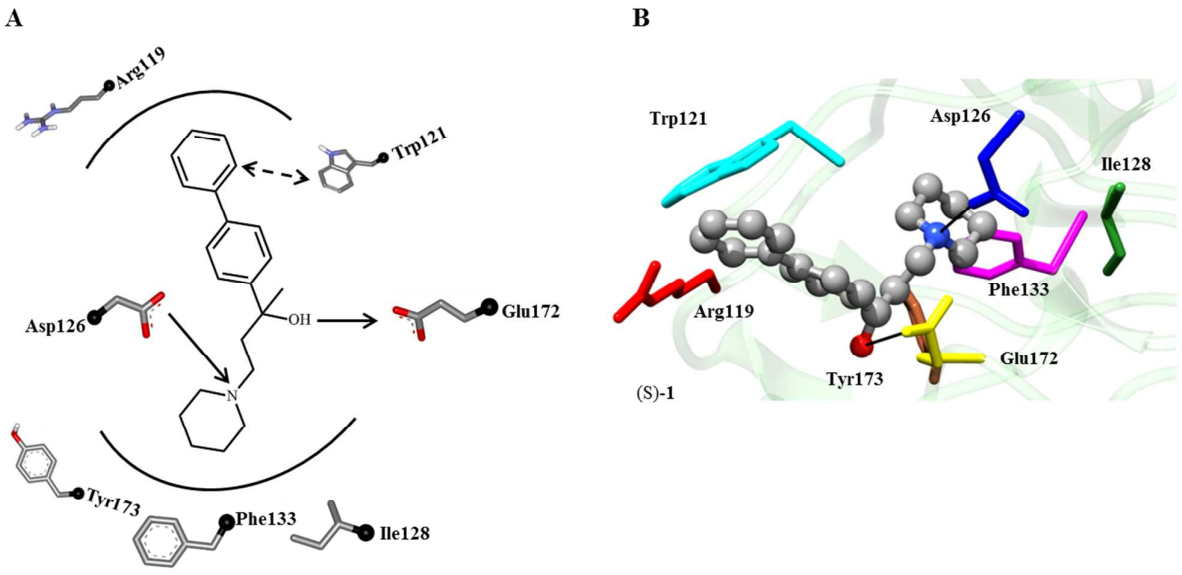


**Fig. 3**. (**A**) Two dimensional schematic representation of postulated interactions between the σ1 receptor and **1**, established by direct affinity measurements. The lines/arrows indicate proposed key interaction between the receptor and its ligand. (**B**) Modeled complex of the $\sigma_1$ receptor with (*S*)-**1** showing the key interactions proposed in the topographical interaction model depicted in part **A**. The main protein residues involved in these interactions are Arg119 (red), Trp121 (cyan), Asp126 (blue), Ile128 (forest green), Glu172 (yellow), and Tyr173 (magenta). The ligand is portrayed in sticks and balls and colored by element, while the protein residues mainly involved in the interaction with (*S*)-**1** are highlighted as colored sticks and labeled. Salt bridge and H-bond interactions are shown as black lines. Water, ions, and counterions are not shown for clarity.

The results of our modeling investigation predict that both enantiomers of **1** can be aptly accommodated within the $\sigma_1$ binding site and establish similar networks of stabilizing interactions with the receptor.

To quantify the overall effect of these interaction, binding free energy calculations were applied and, according to our simulations, both molecules are endowed with similar affinities towards the biological target, with a slight preference of the receptor for the (*S*) enantiomer, as $\Delta G_{bind}$ = -10.81 ± 0.22 kcal/mol for (*R*)-**1** and $\Delta G_{bind}$ = -11.09 ± 0.23 kcal/mol for (*S*)-**1**. The same trend was obtained for all other protein/ligand complexes considered, although compounds **2-5** showed lower affinities towards the $\sigma_1$ receptor with respect to the biphenyl derivatives, as seen from the $\Delta G_{bind}$ values listed in Table 2.

| Compounds | $\Delta H_{bind}$ kcal/mol | -T$\Delta$S kcal/mol | $\Delta G_{bind}$ kcal/mol | $K_i\sigma_{1(calcd)}$* |
|---|---|---|---|---|
| (*R*)-**1** | -23.89 ± 0.09 | -13.08 ± 0.20 | -10.81 ± 0.22 | 12 nM |
| (*S*)-**1** | -24.20 ± 0.08 | -13.11 ± 0.22 | -11.09 ± 0.23 | 7.5 nM |
| (*R*)-**2** | -22.55 ± 0.11 | -12.83 ± 0.21 | -9.72 ± 0.24 | 76 nM |
| (*S*)-**2** | -22.71 ± 0.12 | -12.79 ± 0.20 | -9.92 ± 0.23 | 54 nM |
| (*R*)-**3** | -22.51 ± 0.13 | -12.81 ± 0.23 | -9.70 ± 0.26 | 78 nM |
| (*S*)-**3** | -22.74 ± 0.10 | -12.86 ± 0.19 | -9.88 ± 0.21 | 57 nM |
| (2*R,3S*)-**4** | -20.97 ± 0.08 | -11.88 ± 0.22 | -9.09 ± 0.23 | 219 nM |
| (2*S,3R*)-**4** | -21.46 ± 0.09 | -11.93 ± 0.24 | -9.53 ± 0.26 | 104 nM |
| (2*R,3S*)-**5** | -19.90 ± 0.10 | -11.79 ± 0.21 | -8.11 ± 0.23 | 1.1 μM |
| (2*S,3R*)-**5** | -19.89 ± 0.12 | -11.70 ± 0.18 | -8.19 ± 0.22 | 998 nM |

**Table 2**. Binding free energies $\Delta G_{bind}$ (kcal/mol) and $K_i\sigma_{1(calcd)}$ values for the tested compounds in complex with the $\sigma_1$ receptor. *The calculated $K_i\sigma_1$ were estimated from the corresponding $\Delta G_{bind}$ values using the relationship $\Delta G_{bind} = -RT \ln(1/K_i\sigma_{1(calcd)})$.

To investigate in detail the reason for this behavior, a deconvolution of the enthalpic component ($\Delta H_{bind}$) of the binding free energy into contributions from each protein residue was carried out. As shown in Fig. 4 for compounds (*R*)-**1** and (*S*)-**1**, the stable salt bridge involving Asp126 is responsible for comparable stabilizing contribution of −2.15 kcal/mol and −2.19 kcal/mol, respectively (average dynamic length (ADL) = 4.11 ± 0.05 Å for (*R*)-**1** and ADL= 4.08 ± 0.06 Å for

(*S*)-**1**). Furthermore, the substantial van der Waals and electrostatic interactions contributed, via the aforementioned π interaction, by Arg119 (−0.82 kcal/mol for (*R*)-**1** and −0.88 kcal/mol for (*S*)-**1**) and Trp121 (−1.01 kcal/mol for (*R*)-**1** and −0.98 kcal/mol for (*S*)-**1**), and by the residues belonging to the hydrophobic pocket Ile128, Phe133, and Tyr173 (with a clustered contribution of −3.08 kcal/mol for (*R*)-**1** and −3.04 kcal/mol for (*S*)-**1**), also did not discriminate the affinity of the enantiomers for the receptor. In contrast, the stabilizing effects provided by the permanent hydrogen bond through interaction with Glu172 are dissimilar, as confirmed by the corresponding ADL (2.08 ± 0.06 Å for (*R*)-**1** and 1.92 ± 0.04 Å for (*S*)-**1**, Fig. 4**A**) and, more importantly, the specific $\Delta H_{bind}$ values (−1.01 kcal/mol for (*R*)-**1** and −1.59 kcal/mol for (*S*)-**1,** Fig. 4**B**). These structural and energetical evidences explain the slightly higher affinity of the enantiomer with (*S*) configuration toward the $\sigma_1$ receptor.

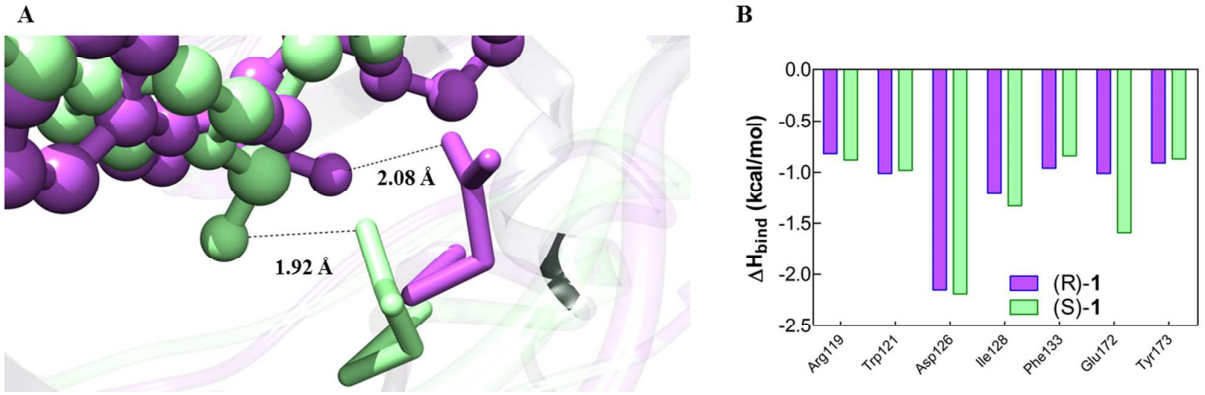


**Fig. 4.** (A) Comparison between the zoomed view of a MD representative snapshot of the hydrogen bond interaction between (R)-**1** (purple) and (S)-**1** (green) with the $\sigma_1$ receptor residue Glu172. The compounds are portrayed as ball-and-stick, while the amino acid is depicted as stick and colored accordingly. (**B**) Per residue energy decomposition for $\sigma_1$ receptor in complex with (R)-**1** (purple) and (S)-**1** (green), showing those residues for which |ΔHbind| > 0.60 kcal/mol.

This *per residue*-based analysis allowed us to better understand and to quantitatively explain the differences in affinity among all compounds of the series. As shown in Table 2, the derivatives **2** and **3** show a decrease in $\Delta G_{bind}$ of about 1 kcal/mol compared to the best ligand **1**. Based on the results of our computational approach both molecules are able to preserve all key interactions with the main $\sigma_1$ residues involved in the binding site (Figs. S3 A and B). Nevertheless, taking the (*S*) enantiomers as reference for our considerations, the replacement of the piperidine portion of (*S*)-**1** with a less bulky N,N-dimethyl group leads to a substantial reduction of the stabilizing contribution afforded by the $\sigma_1$ amino acids Ile128, Phe133, and Tyr172 which constitute the typical hydrophobic pocket of the $\sigma_1$ binding site (Fig. S4). Actually, if the contribution of the other residues remained comparable to that for (*S*)-**1**, the clustered $\Delta H_{bind}$ of these three residues (-1.36

kcal/mol for (*S*)-**2** and -1.45 kcal/mol for (*S*)-**3**, respectively) would become significantly lower in comparison with the value of the piperidine derivative (-3.04 kcal/mol).

Regarding the constrained derivatives (2*S*,3*R*)-**4** and (2*S*,3*R*)-**5**, the increased structural rigidity leads to a different binding pose with respect to the compounds discussed above. As already shown in other studies on $\sigma_1$ ligands,[25f,30] to comply with the pharmacophoric requirements upon target binding these molecules must adopt a reverse orientation into the hydrophobic binding pocket (Figs. S3 C and D). Therefore, the arylpyrrolidinol derivative (2*S*,3*R*)-**4** exhibits a moderate binding affinity ($K_i\sigma_{1(calcd)}$ = 104 nM, Table 2) since its naphthyl moiety can still be encased in the binding pocket by establishing favorable interactions with the involved $\sigma_1$ residues. As a result of this binding pose, the interaction profile of Ile128, Phe133, and Tyr172 with (2*S*,3*R*)-**4** is very similar to that of compound (*S*)-**1** (Fig. S4). However, the structure of this compound prevents it to establish other stabilizing interactions: indeed, we detected a drastic loss in the stabilization effect of the salt bridge with Asp126 and of the hydrogen bond with Glu172 (Fig. S4). In addition, the contribution of the $\pi$ interaction with Arg119 and Trp121 was completely abolished (Fig. S3). Finally, the 6-$OCH_3$ substituted compound (2*S*,3*R*)-**5** ranks as the weakest $\sigma_1$ binder of the series, with an estimated affinity in the μM range (Table 2). In fact, the steric hindrance of its methoxyl group prevents the molecule to penetrate deeply in the receptor binding pocket, (Fig, S3 D) with a consequent overall decrease of all binding stabilizing interactions (Fig. S4).

Taken together, our *in silico* studies support our original hypothesis: actually, the presence of an extra pharmacophoric feature in compounds **1-5,** missing in the original compound **RC-33,** leads to an additional interaction of the ligands with the $\sigma_1$ receptor. Importantly, however, the presence of this feature does not afford a meaningful contribution in differentiating binding affinity of enantiomeric ligands. but, at the same time, it seems to be a potential key-requirement for the stereoselective compound interaction with the $\sigma_1$ receptor. In fact, notwithstanding the interaction spectra for (*R*)- and (*S*)-**1** reported in Fig. 4b differ, both qualitatively and quantitatively, from those obtained for (*R*)- and (*S*)-**RC33**[22e], the contribution afforded by each residue involved in ligand binding is somewhat lower in the case of **1** with respect to **RC33**, ultimately resulting in an only slightly lower affinity of **1** for the receptor. Hence, the presence of the additional pharmacophore feature detected for the present series of compounds seems to play an orientational , rather than en energetically role, in the selectivity of $\sigma_1$ for their (*S*) enantiomers.

**Pharmacological evaluation**

The affinities of (*R,S*)-**1-3**, (*2R/S,3S/R*)-**4-5**, (*R*)-**1-3**, (*2R,3S*)-**4-5**, (*S*)-**1-3**, and (*2S,3R*)-**4-5** towards the $\sigma_1$ and $\sigma_2$ receptors were experimentally determined in radioligand receptor binding studies.

In $\sigma_1$ receptor binding assay the test compounds compete with a potent and selective radioligand (i.e. [$^3$H]-(+)-pentazocine) for the respective binding site. Nonspecific binding was recorded in the presence of cold non-radiolabeled (+)-pentazocine in large excess. Membrane preparations from guinea pig cerebral cortex homogenates served as receptor source. In the $\sigma_2$ assay, membrane preparations of rat liver served as the source for $\sigma_2$ receptors. The nonselective radioligand [3H]DTG was employed in the $\sigma_2$ assay because no $\sigma_2$-selective radioligands are commercially available yet. To mask the $\sigma_1$ receptors, an excess of non-tritiated (+)-pentazocine was added to the assay solution, while a high concentration of non-tritiated DTG was used to determine nonspecific binding. In Table 3 the $\sigma_1$ and $\sigma_2$ receptor affinities of all tested compounds are summarized and compared with affinities of racemic and enantiomeric **RC-33**[22e] as reference compounds. With the only exception of arylpyrrolidinol **5,** which is a weak $\sigma_1$ receptor binder, all compounds generally showed an interesting $\sigma_1$ affinity, in accordance with our *in silico* predictions (Table 2). Most importantly, the (*S*)-configured enantiomers at the stereogenic center directly linked to the aromatic moiety exhibit a preferential interaction with the target protein, thus suggesting that the interaction with the receptor is stereoselective. This is particularly evident for (*S*)-**1**, which shows an eudismic ratio of about 8 and represents the compound with both the highest affinity and selectivity toward $\sigma_2$ receptors among all molecules investigated ($Ki\sigma_1$ = 4.7 ± 0.3 nM, $Ki\sigma_2/Ki\sigma_1$= 382, Table 3).

| Compound | $K_i\sigma_1$ (nM) ± SEM | $K_i\sigma_2$ (nM) ± SEM |
|---|---|---|
| (*R,S*)-**RC-33** | 0.9 ± 0.3 | 103 ± 10 |
| (*R*)-**RC-33** | 1.8 ± 0.1 | 45 ± 16 |
| (*S*)-**RC-33** | 1.9 ± 0.2 | 98 ± 64 |
| (*R,S*)-**1** | 6.57 ± 0.2 | 34.6 ± 47 |
| (*R*)-**1** | 39 ± 8 | 4.3 µM ± 315 |
| (*S*)-**1** | 4.7 ± 0.3 | 1.8 µM ± 288 |
| (*R,S*)-**2** | 77 ± 23 | 66 ± 13 |
| (*R*)-**2** | 205 ± 60 | 651± 67 |
| (*S*)-**2** | 63 ± 39 | 75 ± 5 |
| (*R,S*)-**3** | 41 ± 11 | 97± 18 |
| (*R*)-**3** | 51 ± 14 | 133 ± 63 |
| (*S*)-**3** | 25 ± 4 | 1.1 µM ± 223 |
| (2*R,S/3S,R)*-**4** | 65 ±18 | 366 ± 64 |
| (2*R,3S*)-**4** | 86 ± 16 | 94 ± 23 |
| (2*S,3R*)-**4** | 26 ± 2 | 432 ± 53 |
| (2*R,S/3S,R)*-**5** | 1.9 µM ± 304 | 1.5 µM ± 219 |

| | | |
|---|---|---|
| (2*R,3S*)-**5** | 1.5 μM ± 226 | 1.2 μM ± 212 |
| (2*S,3R*)-**5** | 1.2 μM ± 257 | 1.9 μM ± 293 |

**Table 3.** Binding affinity of the compounds toward $\sigma_1$ receptor. Values are means ± SEM of three experiments.

Racemic and enantiomeric **1** were then selected for further investigation in our validated PC12 cell model of neuronal differentiation with the purpose of determining their agonistic/antagonistic profile and investigating the role of chirality on their effect on NGF-induced neurite outgrowth. The range of concentrations for racemic and enantiomeric **1** was chosen according to our previous assays[22c] performed on **RC-33**. Both (*S*)-**1·D-tartrate** and (*R,S*)-**1·DL-tartrate** displayed a $\sigma_1$ agonistic profile, consistently and significantly potentiating NGF-induced neurite outgrowth at concentrations of 2.5 and 5 μM ($p=0.05$ and $p<0.05$, respectively, vs. NGF alone for (*R,S*)-**1**; $p< 0.01$ and $p<0.005$, respectively, vs. NGF alone for (*S*)-**1**, Fig. 5). Consistently, the effect of these compounds was totally blocked by co-administration of the selective $\sigma_1$ antagonist NE-100. On the contrary, (*R*)-**1·L-tartrate** did not affect the percentage of cells with neurite outgrowth with respect to NGF alone (Fig. 5). Importantly, (*S*)-**1·D-tartrate** resulted more effective than the corresponding racemate in promoting NGF induced neurite outgrowth ($p<0.01$ vs (*R,S*)-**1**, Fig.5).

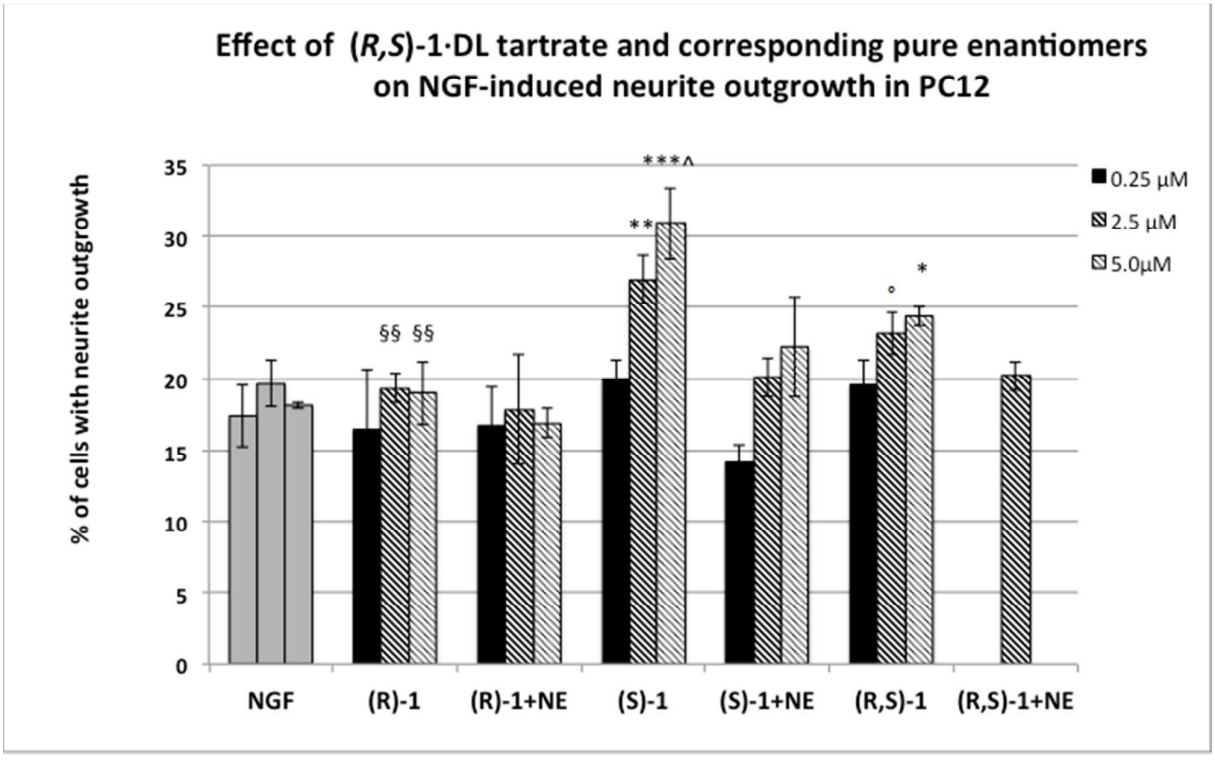


**Fig. 5.** Effect of $\sigma_1$ receptor ligands (*R,S*)-**1·DL-tartrate** and corresponding enantiomers on NGF-induced neurite outgrowth. Co-administration of NE-100 selective $\sigma_1$ receptor antagonist totally blocked the potentiating effect of (*R,S*)-**1** and (*S*)-**1** compounds. Histograms represent the mean ± SEM of at least three different experiments performed in duplicate. ***= $p<0.005$; **= $p< 0.01$; *=$p<0.05$; °=$p=0.05$ vs NGF alone. ^=$p<0.01$ vs (*R,/S*)-**1**; §§= $p< 0.01$ vs (*S*)-**1**.

Taken together, these results show that (*S*)-**1·D-tartrate** is the eutomer. Indeed it enhances NGF-induced neurite outgrowth and its efficacy is greater than (*R,S*)-**1·DL-tartrate,** while (*R*)-**1·L-tartrate** is not effective in promoting NGF induced neurite outgrowth in PC12 cells at the same concentrations.

**Conclusion**

The stereoselectivity of the ligand binding to $\sigma_1$ receptor remains one of the obscure yet intriguing aspects of the activity of this enigmatic transmembrane protein. In this paper, to enrich our knowledge of the structural origins of the enantioselective interaction of $\sigma_1$ ligands we studied the enantiomeric compounds **1-5** structurally related to the potent $\sigma_1$ agonist **RC-33**. According to the latest and more specific $\sigma_1$ receptor 3D pharmacophore models and with respect to the reference ligand **RC-33** (for which the interaction with its target receptor is not dependent on the absolute configuration), compounds **1-5** present an additional pharmacophoric feature: an hydrogen bond center. Our *in silico* analysis of the binding modes and interactions between compounds **1-5** and the $\sigma_1$ receptor revealed that, for these molecules, four major intermolecular interactions are involved in stabilizing ligand binding within the receptor binding pocket. Among those, the extra hydrogen bond interaction - missing in the **RC-33**/$\sigma_1$ receptor complex - plays a role in mild enantiomeric binding discrimination. Interestingly, the mechanism of enantiomer recognition is typically described assuming that three[31] or four[32] key interactions are necessary to distinguish one enantiomer from the other. Thus, our results seem to be in line with this view. Accordingly, for all studied compounds, a weak (about two) to moderate (about eight) stereoselectivity in the interaction with the $\sigma_1$ receptor was observed and (*S*)-**1** was found to be the most active compound of the entire series ($K_i\sigma_1$ = 4.7 nM, eudismic ratio = 8). In summary, we showed that $\sigma_1$ receptor exhibits enantiopreference toward compounds characterized by (*S*)-configuration at the stereogenic center bearing the aromatic moiety only when the alcoholic group is present at the chiral center. Although a more robust and populated data set of compounds is undoubtedly needed to verify our hypothesis, we postulate that an heterogroup at the chiral center is required for a $\sigma_1$-ligand interaction to be stereoselective. An effort to corroborate this claim is ongoing in our laboratories.

Regarding the effect in promoting neurite outgrowth, the results of the functional assays related to **1** demonstrated that the chirality of the molecule affects the biological activity; indeed (*S*)-**1** enhances NGF-induced neurite outgrowth and, also, its efficacy is greater than (*R,S*)-**1**. Most importantly (*R*)-**1** is not effective in potentiating NGF-induced neurite outgrowth at the tested concentrations.

Altogether our observations provide further insights into the role of chirality in the $\sigma_1$ receptor-ligand interaction and represent a step-forward in future development of more specific and effective $\sigma_1$ agonists.

**Author contribution**

Simona Collina, Sabrina Pricl and Daniela Curti conceived the work and contributed in reviewing the whole manuscript. S.C. was also responsible for the correctness of the whole studies. Daniela Rossi was responsible for the design of the experimental work and for data analysis of the whole study and wrote the manuscript. Annamaria Marra and Marta Rui performed the synthesis and chiral resolution of compounds (A.M. also contributed to the writing of the manuscript). Erik Laurini, Maurizio Fermeglia and Sabrina Pricl were responsible for the in silico studies (E.L also contributed the writing of molecular modeling section). Dirk Schepmann, Bernhard Wuensch Marco Peviani and Daniela Curti were responsible for biological investigations (D.S and B.W: binding assays; D.C. and M. P.: NGF-induced neurite outgrowth investigations) and contributed to the writing of the biological section.

**Acknowledgements**

D.R., S.C., M.P., and D.C. gratefully acknowledge financial support from ARISLA (Grant SaNet-ALS). E.L., M.F., and S.P. gratefully acknowledge financial support from ESTECO s.r.l. (Gran DDOS). Access to CINECA supercomputing facility was granted through the sponsored Italian Super Computing Resource Allocation (ISCRA), projects INSIDER and SIMBIOSY (to E.L. and S.P.).

**References:**

(1) W.R Martin, C.E. Eades, J.A. Thompson, R.E. Huppler, P.E. Gilbert, *J. Pharmacol. Exp. Ther.*, 1976, **197**, 517–532.

(2) W.D. Bowen, *Pharm. Acta Helv*., 2000, **74**, 211–218.

(3) S.B. Hellewell, W.D. Bowen, *Brain Res.,* 1990, **527**, 235–236.

(4) Y. Itzhak, I. Stein, *Brain Res*., 1991, **566**, 166–172.

(5) R Quirion, W.D. Bowen, Y. Itzhak, J. L. Junien, J.M. Mustacchio, R.B. Rothman, T.P. Su, S.W. Tam, D. P. Taylor, *Trends Pharmacol. Sci*., 1992, **13**, 85–86.

(6) S. McLean, E. Weber, *Neuroscience,* 1988, **25**, 259–269.

(7) R.R. Matsumoto, M.K. Hemstreet, N.L. Lai, A. Thurkauf, B.R. De Costa, K.C. Rice, S.B. Helleweel, W.D. Bowen, J. M. Walker, *Biochem. Behav*., 1990, **36**, 151–155.

(8) G. Alonso, V.L. Phan, I. Guillemain, M. Saunier, A. Legrand, M. Anoal, T. Maurice, *Neuroscience,* 2000, **97**, 155-170.

(9) V.L. Phan, G. Alonso, F. Sandillon, A. Privat, T. Maurice, *Soc. Neurosci. Abstr*., 2000, **26**, 2172.

(10) S. Collina, R. Gaggeri, A. Marra, A. Bassi, S. Negrinotti, F. Negri, D. Rossi, *Exp. Opin. Ther. Patent*, 2013, **23**(5), 597-613.

(11) T. Maurice, T.P. Su, *Pharmacol. Ther*., 2009, **124,** 195-206.

(12) S. K. Kulkarni, A. Dhir, *Expert Rev. Neurother*., 2009, **9**, 1021-1034.

(13) J. E. Bermack, G. *J.* Debonnel, *Pharmacol. Sci.,* 2005, **97**, 317-336.

(14) S. H. Snyder, B. L. Largent,. *J. Neuropsychiatry Clin. Neurosci*., 1989, **1**(1), 7-15.

(15) A.A. Luty, J.B. Kwok, C. Dobson-Stone, C. T. Loy, K.G. Coupland, H. Karlstrom, T. Sobow, J. Tchorzewska, A. Maruszak, M. Barcikowska, P.K. Panegyres, C. Zekanowski, W.S. Brooks, K. L. Williams, I.P. Blair, K.A. Mather, P.S. Sachdev, G. M. Halliday, P. R. Schofield, *Ann. Neurol*., 2010, **68**, 639-649.

(16) M. Peviani, E. Salvaneschi, L. Bontempi A. Petese, A. Manzo, D. Rossi, M. Salmona, S. Collina, P. Bigini, D. Curti, *Neurobiol. Dis.,* 2014, **62**, 218-232.

(17) T. Hayashi, R. Rizzuto, G. Hajnoczky, T.P. Su, *Trends Cell Biol*., 2009, **19**, 81-88.

(18) T. Hayashi, Z. Justinova, E. Hayashi, G. Cormaci, T. Mori, S.Y. Tsai, C. Barnes, S.R. Goldberg, T.P. Su, *J. Pharmacol. Exp. Ther*., 2010, **332**, 1054-1063.

(19) T. Hayashi, T.P. Su, J. Pharmacol. Exp. Ther., 2003, **306**, 726-733.

(20) T. Hayashi, S. Y. Tsai, T. Mori, M. Fujimoto, T.P. Su, *Expert Opin. Ther. Targets,* 2011, **15**, 557-577.

(21) J.M. Walker, W.D. Bowen, F.O. Walker, R.R. Matsumoto, B. De Costa, K.C. Rice, *Pharmacol. Rev,.* 1990, **42**, 355-402.

(22) (a) S. Collina, G. Loddo, M. Urbano, L. Linati, A. Callegari, F. Ortuso, S. Alcaro, C. Laggner, T. Langer, O. Prezzavento, G. Ronsisvalle, O. Azzolina, *Bioorg. Med. Chem*., 2007, **15**, 771-783; (b) D. Rossi, M. Urbano, A. Pedrali, M. Serra, D. Zampieri, M.G. Mamolo, C. Laggner, C. Zanette, C. Florio, D. Shepmann, B. Wünsch, O. Azzolina, S. Collina, *Bioorg. Med. Chem.,* 2010, **18**, 1204-1212; (c) D. Rossi, A. Pedrali, M. Urbano, R. Gaggeri, M. Serra, L. Fernandez, M. Fernandez, J. Caballero, S. Rosinsvalle, O. Prezzavento, D. Shepmann, B. Wünsch, M. Peviani, D. Curti, O. Azzolina, S. Collina, *Bioorg. Med. Chem*., 2011, **19**, 6210-6224; (d) D. Rossi, A. Marra, P. Picconi, M. Serra, L. Catenacci, M. Sorrenti, E. Laurini, M. Fermeglia, S. Pricl, S. Brambilla, N. Almirante, M. Peviani, D. Curti, S. Collina, *Bioorg. Med. Chem*., 2013, **21**, 2577-2586; (e) D. Rossi, A. Pedrali, R. Gaggeri, A. Marra, L. Pignataro, E. Laurini, V. DalCol, M. Fermeglia, S. Pricl, D.

Schepmann, B. Wünsch, M. Peviani, D. Curti, S. Collina, *Chem. Med. Chem.,* 2013, **8**, 1514-1527; (f) D. Rossi, A. Pedrali, A. Marra, L. Pignataro, D. Schepmann, B. Wünsch, L. Ye, K. Leuner, M. Peviani, D. Curti, O. Azzolina, S. Collina, *Chirality,* 2013, **25**, 814-822.

(23) D. Zampieri, M.G. Mamolo, E. Laurini, C. Zanette, C. Florio, S. Collina, D. Rossi, O. Azzolina, L. Vio, *Eur. J. Med. Chem*., 2009, **44**, 124-130.

(24) T. Schläger, D. Shepmann, K. Lehmkuhl, J. Holenz, J. M. Vela, H. Buschmann, B. Wünsch, *J. Med. Chem*., 2011, **54**(19), 6704-6713.

(25) (a) R.A. Glennon, S.Y. Ablordeppey, A.M. Ismaiel, M.B. El-Ashmawy, J.B. Fischer, K.B. Howie, *J. Med. Chem*., 1994, **37**, 1214-1219; (b) T. M. Gund, J. Floyd, D.J. Jung, *Mol. Graphics Modell*., 2004, **22**, 221-230; (c) C. Laggner, C. Schieferer, B. Fiechtner, G. Poles, R.D. Hoffmann, H. Glossmann, T. Langer, F.F. Moebius. *J. Med. Chem.,* 2005, **48**, 4754-4764; (d) D. Zampieri, M.G. Mamolo, E. Laurini, C. Florio, C. Zanette, M. Fermeglia, P. Posocco, M.S. Paneni, S. Pricl, L. Vio, *J. Med. Chem*., 2009, **52**, 5380-5393; (e) C. Oberdorf, T.J. Schmidt, B. Wünsch, *Eur J Med Chem*., 2010 **45**(7), 3116-24; (f) C. Meyer, D. Schepmann, S. Yanagisawa, J. Yamaguchi, V. Dal Col, E. Laurini, K. Itami, S. Pricl, B. Wuensch, , *J. Med. Chem.,* 2012, **55**, 8047-8065.

(26) R. Kekuda, P.D. Prasad, J.Y. Fei, F.H Leibach, V. Ganapathy, *Biochem. Biophys. Res. Commun*., 1996, **229**, 553–558.

(27) R. A. Glennon, *Mini-Rev. Med. Chem*., 2005, **5**, 927–940.

(28) (a) O. Azzolina, S. Collina, G. Brusotti, D. Rossi, A. Callegari, L. Linati, A. Barbieri and V. Ghislandi, *Tetrahedron: Asymmetry*, 2002, **13**, 1073-1081; (b) S. Collina, O. Azzolina, D. Vercesi, M. Sbacchi, M. A. Scheideler, A. Barbieri, E. Lanzac and V. Ghislandi, *Bioorg. Med. Chem*., 2000, **8**, 1925-1930; (c) S. Collina, O. Azzolina, D. Vercesi, G. Brusotti, D. Rossi, A. Barbieri, E. Lanza, L. Mennuni, S. Alcaro, D. Battaglia, L. Linati, V.Ghislandi, *Il Farmaco,* 2003, **58,** 939-946; (d) S. Collina, D. Rossi, G. Loddo, A. Barbieri, E. Lanza, L. Linati, S. Alcaro, A. Gallelli, O. Azzolina, *Bioorg. Med. Chem*., 2005, **13**, 3117-3126.

(29) (a) J. Srinivasan, T.E. Cheatham, P. Cieplak, P.A. Kollman, D.A. Case, *J Am Chem Soc.,* 1998; **120**, 9401-9409. (b) P.A. Kollman, I. Massova, C. Reyes, B. Kuhn, S. Huo, L. Chong, M. Lee, T. Lee, Y. Duan, W. Wang, O. Donini, P. Cieplak, J. Srinivasan, D.A. Case ,T.E. Cheatham, *Acc Chem Res.,* 2000, **33**, 889-897.

(30) (a) Laurini, E.; Dal Col, V.; Mamolo, M. G.; Zampieri, D.; Posocco, P.; Fermeglia, M.; Vio, V.; Pricl, S. *ACS Med. Chem. Lett,.* 2011, **2**, 834-839. (b) Laurini, E.; Marson, D.; Dal Col, V.; Fermeglia, M.; Mamolo, M. G.; Zampieri, D.; Vio, L.; Pricl, S. *Mol. Pharmaceutics,* 2012, **9**, 3107-3126.

(31) Armstrong DW, Ward TJ, Armstrong RD, Beesley TE., Separation of drug stereoisomers by the formation of beta-cyclodextrin inclusion complexes, *Science*, 1986, **232**(4754), 1132-1135.
(32) Mesecar AD1, Koshland DE Jr. A new model for protein stereospecificity, *Nature*, 2000, **403**(6770), 614-615.

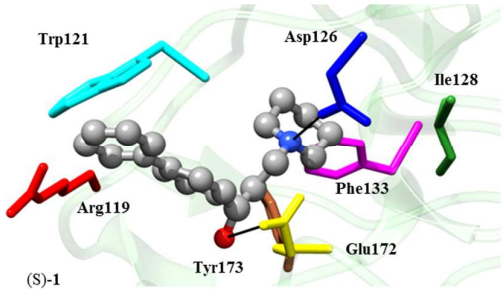


To investigate the role of chirality in the ligand/$\sigma_1$ receptor interaction, a series of enantiomeric arylalkylaminoalcohols and arylpyrrolidinols was evaluated by means of both *in silico* and *in vitro* study.